energies

MDPI

Article

Sewage Sludge-Derived Biochar and Its Potential for Removal of Ammonium Nitrogen and Phosphorus from Filtrate Generated during Dewatering of Digested Sludge

Katarzyna Wystalska and Anna Grosser *

Faculty of Infrastructure and Environment, Czestochowa University of Technology, 42-200 Czestochowa, Poland; katarzyna.wystalska@pcz.pl

* Correspondence: anna.grosser@pcz.pl

Abstract: Utilizing waste, such as sewage sludge, into biochar fits the circular economy concept. It maximizes the reuse and recycling of waste materials in the wastewater treatment plant. The experiments were conducted to assess: (1) the impact of the temperature on the properties of biochar from sewage sludge (400 °C, 500 °C, 600 °C, 700 °C); (2) how the physical activation (CO_2, hot water) or chemical modification using ($MgCl_2$, KOH) could affect the removal of ammonia nitrogen and phosphorus from filtrate collected from sludge dewatering filter belts or synthetic solution, wherein the concentration of ammonium nitrogen and phosphorus were similar to the filtrate. Based on the Brunner–Emmett–Teller (BET) surface and the type and concentration of surface functional groups for the second stage, biochar was selected and produced at 500 °C. The modification of biochar had a statistically significant effect on removing nitrogen and phosphorus from the media. The best results were obtained for biochar modified with potassium hydroxide. For this trial, 15%/17% (filtrate/synthetic model solution) and 72%/86% nitrogen and phosphorus removal, respectively, were achieved.

Keywords: biochar; sewage sludge; filtrate from dewatering; removal of ammonium nitrogen; removal of phosphorus; pyrolysis; digestate

check for updates

Citation: Wystalska, K.; Grosser, A. Sewage Sludge-Derived Biochar and Its Potential for Removal of Ammonium Nitrogen and Phosphorus from Filtrate Generated during Dewatering of Digested Sludge. *Energies* **2024**, *17*, 1310. https://doi.org/10.3390/en17061310

Academic Editor: Marcin Dębowski

Received: 20 February 2024
Revised: 2 March 2024
Accepted: 6 March 2024
Published: 8 March 2024

Copyright: © 2024 by the authors. Licensee MDPI, Basel, Switzerland. This article is an open access article distributed under the terms and conditions of the Creative Commons Attribution (CC BY) license (https://creativecommons.org/licenses/by/4.0/).

1. Introduction

Municipal wastewater treatment plants generate large amounts of waste in wastewater treatment processes. Among them, sewage sludge has excellent material and energy potential. According to the circular economy concept, this waste can be converted into value-added products [1] and put into environmental circulation [2]. The use of pyrolysis for its transformation can result in the acquisition of biochar—a material with specific properties characterized by a wide range of applications. Porosity, specific surface area, cation exchange capacity, stability, and the presence of significant amounts of C, N or P determine the possibilities of using biochar in many branches of engineering or environmental protection [2–14]. The characteristic features of biochar mainly depend on the type of raw material from which it was produced and the applied temperature of the pyrolysis process [15–18], affecting, among others, the specific surface area of biochar and the type of surface functional groups [19]. For these reasons, it is important to combine raw material selection, process temperature, heating time, and reaction time [20,21] to achieve the expected product with properties that allow the desired effect.

The results of many researchers [22–24] demonstrate an adsorption potential of biochar from sewage sludge. For instance, Tang et al. [24] showed that biochar produced from digested sewage sludge is a promising adsorbent that can remove ammonium from municipal wastewater. The highest adsorption capacity was displayed by biochar produced at 450 °C, probably due to the specific surface area and the presence of specific functional groups. In turn, the possibility of using biochar from sewage sludge for the recovery of

ammonium in urine was also demonstrated by Bai et al. [22]; they used biochar enriched in this way for soil conditioning.

Unfortunately, the low performance of sludge-based sorbents limits their practical use [25]. Therefore, these adsorbents are modified accordingly by controlling key pyrolysis parameters or using physical and chemical activation techniques [2,11,26]. This is due to the fact that changes in pyrolysis and activation conditions directly impact the adsorbent properties, adsorption capacity, and pollutant removal mechanism of sludge-based adsorbents [27]. For instance, Xu et al. [28] showed that the high temperature of the biochar production process is not always correlated with high adsorption capacity. Biochar from rice straw obtained by pyrolysis at 500 °C had a higher adsorption capacity of NH_4^+-N than biochar obtained at 700 °C. According to the authors, the C/H ratio was an essential factor influencing the sorption of ammonium ions. In turn, Jiang et al. [23] demonstrated that biochar with a high Mg content could be a valuable adsorbent of ammonium nitrogen (NH_4^+-N) and phosphorus from aqueous solutions, with the nature of the substrate from which the biochar was produced is of significant importance. In addition, their research has shown that the adsorption of N and P was strongly correlated with the Mg content, and the total pore volume and the specific surface area showed a weak and moderate correlation, respectively. Moreover, the adsorption of ions was based on magnesium phosphate precipitation reactions.

Therefore, studies were carried out aimed to produce, characterize, and assess the suitability of biochar from sewage sludge for the recovery of nitrogen and phosphorus from wastewater produced by dewatering sewage sludge on belt filter presses. This fits in with current research trends because the development of research on using biochar to remove nitrogen and phosphorus from wastewater or other media is currently highly desirable [29]. Significant amounts of nitrogen and phosphorus characterize the leachates generated by sewage sludge dewatering processes. A common practice in wastewater treatment plants is the return of wastewater to the technological process line of the treatment plant [30]. Such actions may cause a disturbance in the technological processes carried out in the wastewater treatment plant and the non-use of valuable nutrients present in them.

There is no shortage of examples in the literature that combining anaerobic digestion and pyrolysis is a promising, environmentally friendly and forward-looking approach to waste treatment, including sewage sludge, allowing the final product (biochar) to be used in numerous applications. However, this research mainly focuses on (1) maximizing energy recovery through pyrolysis of solid digestate, (2) upgrading biogas by biochar, and (3) enhancing the stability of the anaerobic digestion process by biochar addition to the digester [31]. Lack of work that combines the two processes allows waste management improvements at a wastewater treatment plant in line with the idea of a circular economy. For this reason, we decided to focus on the possibility of using pyrolysis to transform the digestate into a valuable product that can then be used at a wastewater treatment plant to solve the issue of pretreatment of leachate (filtrate) after digestate dewatering, which is a very important issue from the point of view of the wastewater treatment plant operator.

2. Materials and Methods

2.1. Experimental Procedure

The reported experiment was divided into two stages, implemented consecutively, as shown in Figure 1. During stage 1, biochar was prepared. Based on their characteristics, one biochar was selected for the next stage. In the 2nd stage, the adsorption of ammonia, nitrogen, and phosphorus from different solutions was performed to determine the practical application of the biochar produced in the first stage.

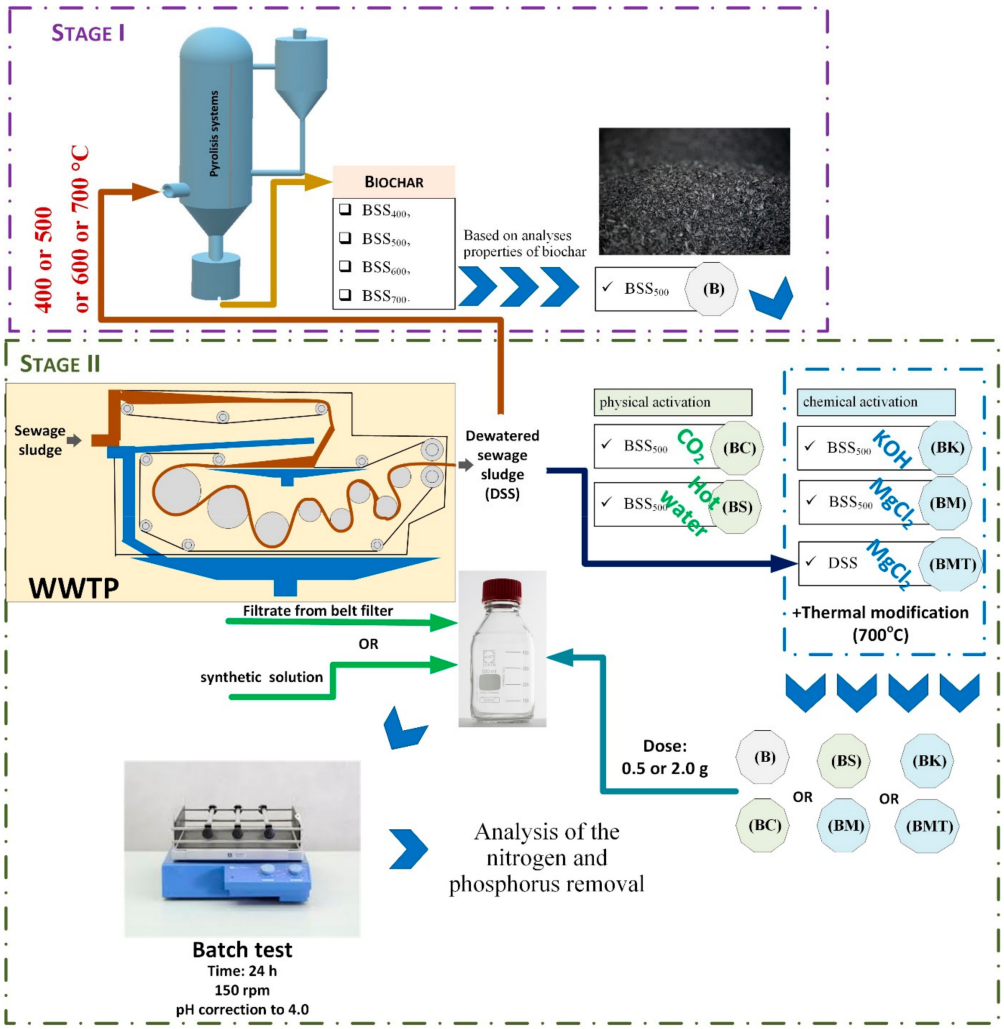


Figure 1. Scheme of experiment.

2.2. Raw Materials for Biochar Production

Dried sewage sludge (SS) (digestate after anaerobic digestion) was taken from a wastewater treatment plant located in southern Poland and used to produce biochar. In the technology used there for the processing of municipal sewage sludge, after the dewatering process (belt filter presses), the sludge is directed to a drying and granulation installation in which it is dried to approximately 90–95% of dry mass. Table 1 shows the selected properties of the sewage sludge, among others, pH, moisture (M), ash, total carbon (C), and nitrogen content (NK). The SS were characterized by a neutral pH and a high ash content of approximately 55%. The carbon content is approximately 33%, and the total nitrogen content is approximately 4.47%.

Table 1. Selected properties of sewage sludge.

	pH_{H2O}	M%	Ash%	C%	N_K%
SS	7.02 ± 0.22	6.25 ± 0.59	55.18 ± 0.31	33.11 ± 1.01	4.47 ± 0.52

2.3. Preparation of Biochar

The substrates were subjected to thermal conversion in a pyrolysis reactor (PRW-S100x780/11 in a nitrogen atmosphere (5 L/min). The Polish company Czylok (Jastrzębie-Zdrój, Poland) manufactured the pyrolysis reactor for the Czestochowa University of Technology. The heating temperatures of the substrate were: 400 °C, 500 °C, 600 °C, and

700 °C. The heating times of samples were 120 min for temperatures of 400 °C and 500 °C and 150 min for temperatures of 600 °C and 700 °C, respectively. The retention time was 60 min. After the pyrolysis process was completed, the samples were left in the reactor until they reached room temperature. Biochar samples were stored in tightly closed containers at room temperature. The biochars produced in the pyrolysis of SS are denoted as BSS_{400}, BSS_{500}, BSS_{600}, and BSS_{700}.

2.4. Modification of Biochar

Biochar modification (BSS_{500}) was carried out using physical and chemical methods. During physical activation, biochar was heated at 750 °C (heating time 150 min, reaction time 60 min) in a CO_2 atmosphere (4 L/min). The biochar is denoted as BC. The second method of physical activation was hot water modification. An amount of 200 g of biochar was flooded with 2 L of distilled water and kept boiling for one hour. The biochar was then rinsed with distilled water and dried to constant weight for 24 h at 105 °C. The biochar is denoted as BS.

Biochar has also been modified using chemical reagents such as KOH and $MgCl_2$. Biochar was mixed with KOH at a weight ratio 1:1, then heated at 700 °C (heating time 150 min, reaction time 60 min) in a nitrogen atmosphere (5 L/min). Then, the process of neutralizing HCl and rinsing with distilled water to pH ~5 was used. The biochar is denoted as BK. In the modification process using $MgCl_2$, biochar and the dried sewage sludge (DSS) were treated. An amount of 20 g of biochar and 20 g of sludge were flooded with 200 mL (1 M) of $MgCl_2$, shaken for one hour (150 rpm) and left for 24 h. The resulting products were dried at 105 °C and heated at 500 °C (heating time 120 min, reaction time 60 min) in a nitrogen atmosphere (5 L/min). The modified biochar is denoted as BM, and the modified DSS is denoted as BMT.

2.5. Batch Adsorption Experiments

The experiment of removing ammonium nitrogen and phosphorus was carried out using biochar produced at 500 °C. The experiment was carried out using non-modified biochar and biochar modified using chemical and physical methods (Figure 1). The experiment used the filtrate after dewatering sewage sludge on belt filter presses and the synthetic solution. Stock solutions were prepared using NH_4Cl and KH_2PO_4. The volumes of the stock solution have been selected so that the synthetic solution composition is close to the actual filtrate. The selected properties of the filtrate and the synthetic solution are shown in Table 2.

Table 2. Characteristic of selected properties of filtrate and synthetic solution.

Parameter	The Filtrate from the Belt Filter	Synthetic Solution
pH, -	7.75	4.73
$N\text{-}NH_4^+$, mg/L	864.27 ± 6.47	890.40 ± 14.82
P, mg/L	20.09 ± 0.87	18.95 ± 0.5
NPOC, mg/L	189.20 ± 1.72	-

The tested biochar (in two dosages of 0.5 g and 2.0 g) was inundated with 100 mL of actual filtrate or synthetic solution. Each time, the pH has been adjusted to pH = 4. The prepared mixtures were then shaken on the shaker for 24 h (at 150 rpm). Eluates were filtered, and their ammonium nitrogen and phosphorus concentrations were determined.

The adsorption capacity (q_m) of ammonia nitrogen and phosphorus on tested solutions was calculated using the following equation:

$$q_m = \frac{c_0 - c_{eq}}{m \times V} \left(\frac{mg}{g} \right) \quad (1)$$

The percentage of ammonia nitrogen, and phosphorus immobilized by the tested mixtures was calculated using the equation [32]:

$$Removal = \frac{c_0 - c_e}{c_0} \times 100\ (\%) \quad (2)$$

where

c_0—the initial concentration of the ammonia nitrogen or phosphorus in solution, mg/L;
c_{eq}—the equilibrium concentration of the ammonia nitrogen and phosphorus in solution, mg/L;
V—the volume of the solution, L;
m—the weight of biochar, g.

2.6. Physicochemical and Physical Analyses

The sewage sludge and the obtained biochars were analyzed for moisture content (M) (by oven drying at 105 °C for 48 h using drying ovens SL115, POL-EKO, Wodzisław Śląski, Poland) and ash (combusting the sample at 550 °C for two h in a muffle furnace FCF-12 SHM, Czylok, Jastrzębie-Zdrój, Poland; by [33]). Sewage sludge was analyzed for total carbon content (by Multi N/C, Analytk, Jena, Germany—the high-temperature incineration with detection IR) and Kjeldahl nitrogen content (according to [34]). pH measurement was made by placing 5 g of the sample in three individual beakers and then adding distilled water to each (50 mL). The beakers were shaken for 10 min and then infiltrated. pH was measured by a pH meter. Biochars derived at selected temperatures were analyzed for elemental composition, total organic carbon content, surface area, morphology, and the presence of surface functional groups. The CHNS elemental analysis was performed with the Thermo Scientific™ (Waltham, MA, USA) FLASH 2000 method of dynamic incineration (3–4 independent incineration). Total organic carbon content was indicated by analyzer TOC-5000A (made by Shimadzu, Kyoto, Japan) with SSM 5000 attachment. TOC was indicated by high-temperature incineration (900 °C). Carbon dioxide was measured by infrared spectrometry and expressed as carbon. The Brunner–Emmett–Teller (BET) surface area was indicated by the ASAP 2420. The ASAP 2420 analyzer (company Micromeritics, Norcross, GA, USA) measures single- and multi-point-specific surface areas and the size and distribution of pore solid samples. The analytical techniques included scanning electron microscopy (SEM), which was used to examine the morphology of samples. Surface functional groups were identified by Attenuated Total Reflectance Fourier-transform infrared spectroscopy.

Additionally, the following parameters were analyzed: ammonium nitrogen (N-NH_4^+) (steam distillation, BÜCHI K-355, Flawil, Switzerland), pH (pH meter Cole Parmer Model No. 59002-00, Eaton Socon, UK), and phosphorus (ascorbic acid method, spectrophotometer Hach DR/4000, Loveland, CO, USA) All mentioned analyses were performed according to the APHA Standard Methods for the Examination of Water and Wastewater [35]. All analyses were conducted in triplicate.

2.7. Statistical Analyses

The impact of the type of biochar and the kind of solution on the removal of ammonium nitrogen and phosphorus were estimated based on the analysis of variance (factorial ANOVA). The homogeneity of variances was checked using Levene's test. Data that failed the ANOVA assumptions were analyzed via the Kruskal–Wallis test. ANOVA was performed with at least three replications for each combination of the nominal variables. In the case of ANOVA, when analysis showed that statistically significant data were achieved ($p < 0.05$), a post hoc Tukey honest significant difference (HSD) was used. The statistical estimation was carried out using STATISTICA software (STATISTICA 12 PL, StatSoft, Inc., Tulsa, OK, USA).

3. Results and Discussion

3.1. Biochar Production Efficiency

The pyrolysis process was carried out at temperatures: 400 °C, 500 °C, 600 °C, and 700 °C. As the temperature increased, a decrease in biochar production efficiency was observed (Table 3), which is caused by the loss of water and substances that decompose at high temperatures. The process carried out at a temperature of 400 °C showed the highest efficiency (over 62%). The biochar yield ranging from 49.5 to 63% is at a high level, typical of biochars produced from fecal substrates. The reason for this phenomenon is the higher content of ash (mineral substances) in sewage sludge. In studies [13,15,36,37], the biochar yield achieved at 400 °C was approximately 45%. This value is significantly lower than in our research; however, it concerns the transformation of plant substrates into biochar. The use for the production of biochar in chicken manure allowed the author [19] to achieve a similar yield of approximately 62% (at a pyrolysis temperature of 400 °C). The biochar yield from fecal substrates, e.g., sewage sludge or chicken manure, is usually more significant than the biochar produced from plant substrates. Differences in the biochar production efficiency of substrates of fecal and vegetable origin are due to a higher ash content (inorganic substances) in sewage sludge compared to plant biomass [38]. Song and Guo [16], in their study, achieved the highest efficiency of the pyrolysis process of chicken manure at 300 °C. The biochar yield was then at 60.13%, whereas the process efficiency decreased to 51.52% at 400 °C. Researchers Ruiz-Gomez and others [39] analyzed the pyrolysis process of sewage sludge and fermented cow manure at 525 °C. The conversion of sewage sludge in this case resulted in an efficiency of approximately 51%. By contrast, the pyrolysis yield of fermented manure was approximately 49%. In our case, in a process carried out at a similar temperature level, the production efficiency of biochar from sewage sludge was higher, at approximately 56%. The observed trend is consistent with the results presented by other researchers [16,40–43].

Table 3. Biochar production yields at different temperatures and properties of the biochar produced.

	BSS_{400}	**BSS_{500}**	**BSS_{600}**	**BSS_{700}**
Yield, %	62.41 ± 0.56	56.12 ± 1.05	52.79 ± 0.20	49.33 ± 1.75
pH_{H2O}	7.13 ± 0.07	7.53 ± 0.39	10.76 ± 0.06	11.03 ± 0.15
moisture, %	2.21 ± 0.04	4.08 ± 0.04	3.59 ± 0.06	3.13 ± 0.02
Ash, %	48.13 ± 12.69	63.10 ± 0.47	67.16 ± 0.08	71.43 ± 0.22
C, %	42.40 ± 11.55	26.98 ± 0.25	27.32 ± 0.02	27.07 ± 0.15
H,%	2.59 ± 0.07	1.44 ± 0.00	0.93 ± 0.00	0.59 ± 0.00
N, %	3.22 ± 0.04	2.60 ± 0.01	2.29 ± 0.02	1.40 ± 0.00
S, %	-	-	-	-
TOC, %	27.9 ±7.3	23.5 ± 6.1	27.0 ± 7.2	26.6 ± 6.9
H/C, %	0.73	0.64	0.41	0.26
BET, m^2/g	11.09 ± 0.16	40.97 ± 0.14	43.33 ± 0.24	45.53 ± 0.31

3.2. Characteristics of Selected Biochar Properties

Biochar variants produced by sewage sludge pyrolysis at different temperatures are designated BSS_{400}, BSS_{500}, BSS_{600}, and BSS_{700}. Biochar was subjected to a physicochemical analysis, including determination, among others, of pH, ash, carbon (C), hydrogen (H), nitrogen (N), sulfur (S), and organic carbon (TOC). The results of the analysis are presented in Table 3.

Biochar produced at temperatures of 400 and 500 °C had a pH not exceeding 8. The BSS_{600} and BSS_{700} biochar variants were alkaline and had a pH of 10.76 and 11.03, respectively. The pH values of all biochar variants confirm the trend—also demonstrated in other

studies—of an increase in pH with an increase in the temperature of the pyrolysis process [13,15,16,38]. This effect is associated, among others, with the formation of carbonate and the presence of inorganic alkalis [44].

The determined ash content in biochar was in the range of 48.13–71.43%. The observed increase in the ash content of biochar produced at ever higher temperatures results from the increasing content of inorganic components and residues from the combustion of organic matter [45,46].

An elementary analysis of the C content of biochar showed the presence of this element at approximately 42% for biochar produced at 400 °C. The increase in pyrolysis temperature caused a significant decrease in that value to approximately 27% for biochar produced in the remaining temperatures. The H content decreased as the pyrolysis temperature increased and fell from approximately 2.59% (BSS_{400}) to 0.59% (BSS_{700}). These dependencies are caused by the dewatering of transformed substrates and the loss of H-atoms connected with C as a result of thermal degradation [47]. Changes in the C and H content of biochar from different temperatures determine the value of the H/C ratio, which, as per requirements [48], should not exceed 0.7. For our biochar, this condition is only not met for BSS_{400} biochar. Other biochar variants are characterized by a H/C ratio of 0.64–0.26, indicating deepening carbonization and increased aromaticity [49,50]. These features determine the stability of biochar, including the sorption potential [51,52]. The N content of biochar showed a decreasing trend as the temperature of the pyrolysis process increased. The highest value of 3.22% was determined for biochar produced at 400 °C; for BSS_{700} biochar, this value was only 1.40%. Sulfur in the analyzed biochar has not been determined.

The organic carbon content of obtained biochar fluctuated between 23.5% and 27.9%. However, taking into consideration the European Biochar Certificate [48] requirements for the organic carbon content of biochar used in agriculture, the organic carbon content should be >50% DM. The low organic carbon content in the analyzed biochar does not exclude its other applications.

The produced biochar was characterized by specific surface areas ranging from 11.09 to 45.53 m^2/g (Table 3). The highest BET surface area value was determined when the pyrolysis process was carried out at 700 °C. The temperature of 500 °C was the level at which there was a significant increase in the studied parameter from 11.09 m^2/g (400 °C) to 40.97 m^2/g. This trend also continued with temperatures rising from 600 to 700 °C. As shown by the authors [53], high temperatures of sewage sludge pyrolysis may result in an increase in the value of the specific surface area, from 4.88 m^2/g, for 300 °C, to 34.21 m^2/g for 900 °C. BET surface area value, determined in our research, for $BSS_{700,}$ was significantly higher.

Research results presented by other researchers [16,53–57] show a relationship between the increase in the value of the specific surface area as the temperature of the pyrolysis process increases, which is caused by the removal of volatile substances, resulting in an increase in the volume of micropores [58]. In our research, this trend is not as pronounced, which may be conditioned by a certain heterogeneity of the transformed material.

Biochars produced at different temperatures did not show very significant differences in the BET-specific surface area value. These values were quite low compared, for example, to the BET surface of biochars made from lignocellulosic raw materials, which have a well-developed microporous structure. High ash content in biochar may block the development of specific surface area due to the pores being clogged by inorganic compounds present in the ash. Figure 2 shows the microstructure of the biochar produced. It does not show an expanded microporous structure.

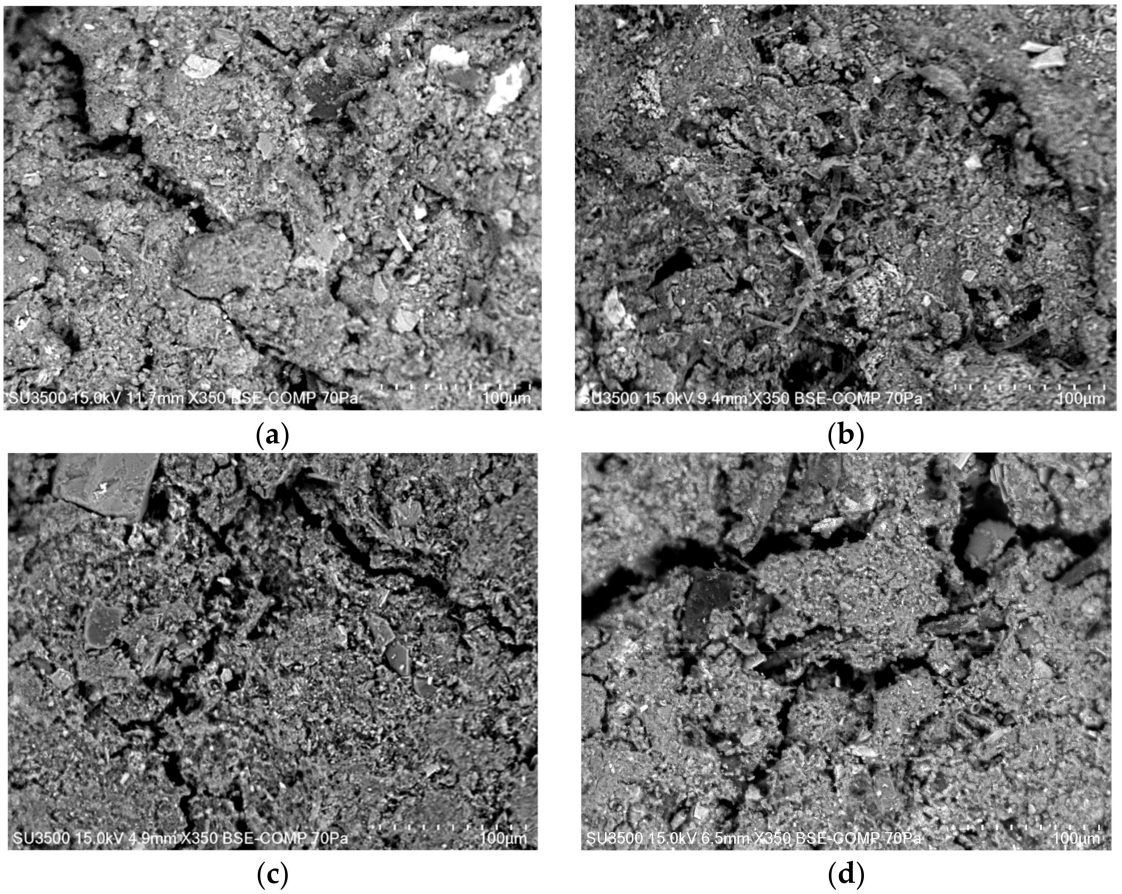


Figure 2. Microstructure of biochar: (**a**) BSS_{400}, (**b**) BSS_{500}, (**c**) BSS_{600}, and (**d**) BSS_{700}.

An analysis of the FTIR spectra (Figure 3) of produced biochar showed the presence of bands corresponding to the OH-stretching vibrations (in the wavelength area, 3329 cm^{-1} to 3340 cm^{-1}) for all biochar variants except BSS_{700}. The absence of OH-stretching vibrations is probably due to, among others, the dewatering of the material and loss of volatile substances, as OH groups are volatile at elevated temperatures. The presence of bands corresponding to the CH-stretching vibrations (occurring in aliphatic compounds [7]) has been determined only in BSS_{400} biochar in 2924 cm^{-1}. The lack of a signal corresponding to these vibrations in other biochar variants produced at higher temperatures was probably due to the rupture of the relatively weak C-H bonds [50,59] and a lack of acidic functional groups that affect the ability of sorption of nutrients [16]. The presence of CH groups in the FTIR spectrum under analysis further confirms the presence of bands occurring in the area 1436 cm^{-1}; this signal is attributed to the deformation modes of these groups [50]. CH-deformation vibrations were also found in BSS_{500} and BSS_{600} (in the areas 1425 and 1438 cm^{-1}), where no CH-stretching vibrations were found. In the FTIR spectra of all analyzed biochar variants, signals from the C=C group stretching vibrations in the area ~1593–1560 cm^{-1} were observed. The intensity of these signals decreases as the temperature of pyrolysis increases. The pyrolysis temperature of 600 °C or higher may cause multiple double C=C bonds to break down, resulting in decreased C=C binding structures in biochar [59]. The observed signals correspond to the wavenumber in the area of approx. 1576 cm^{-1}, may be associated with vibrations of the C=C group in an aromatic ring coupled with the carbonyl C=O group [53]; this may indicate that the resulting products contain in their structure organooxygen structural groups coupled with double C=C bonds in the aromatic rings.

In FTIR spectra of all biochar variants, bands corresponding to CO-stretching vibrations (in the range of ~1020–1031 cm^{-1}) were found, which may be the result of the formation of aromatic ethers due to the inclusion of oxygen atoms in cyclic carbon struc-

tures. The absorption bands at ~1050–850 cm^{-1} can be assigned to C–O stretching modes and O–H deformation in alcohols, phenols, ethers, and esters [53]. The signal corresponding to the CO-stretching vibrations (in the area ~1027 cm^{-1}) present in the BSS_{500} biochar spectrum has the highest intensity of all signals on the spectra of other biochar variants in the analyzed area. This feature, combined with the previously signaled BET surface area value of BSS_{500} biochar, may indicate the most significant sorption potential of various contaminants.

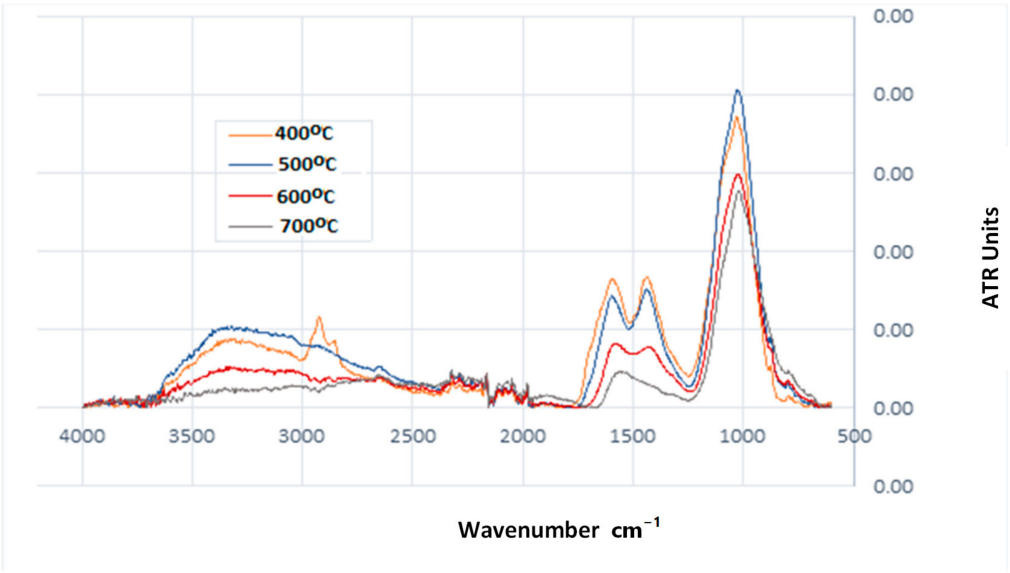


Figure 3. FTIR/ATR spectra of biochar produced at different temperatures (400 °C, 500 °C, 600 °C, and 700 °C.

3.3. Biochar as an Adsorbent for Ammonia Nitrogen/Phosphorus Removal

The practical application of biochar from sewage sludge as nitrogen and phosphorus adsorbent has been tested separately concerning removing these compounds from two liquid media and the adsorption efficiency (Table 4). Such an approach has been chosen because, very often in the literature, both ions are removed simultaneously, although opinions about their interaction are divided. In the literature on the subject, works suggest a reduction in the adsorption of ammonium ions through orthophosphate ions [29].

Table 4. The adsorption capacity for biochar used in this study.

Type of Biochar	Dose, g	qm, mg/g for NH_4^+		qm, mg/g for PO_4^{3-}	
		Filtrate	Synthetic Solution	Filtrate	Synthetic Solution
B	0.5	5.97	6.72	-	0.01
	2	1.68	3.45	0.05	0.27
BC	0.5	7.47	8.21	0.07	0.5
	2	1.12	3.08	0.42	0.48
BS	0.5	6.72	7.47	-	0.17
	2	2.52	2.52	0.27	0.31
BK	0.5	15.31	14.19	1.2	1.33
	2	6.44	7.65	0.72	0.8
BM	0.5	14.56	8.21	-	-
	2	2.89	2.33	0.22	0.47
BMT	0.5	11.57	6.72	-	-
	2	2.89	1.59	-	-

- phosphorus leaching from biochar was noted.

As shown in Figure 4, ammonium nitrogen removal efficiency ranged from 2.53 to 17.19%. The highest adsorption was recorded for potassium-hydroxide-modified carbon. As demonstrated by the factor analysis of variance, the type of medium had no significant statistical effect on ammonium nitrogen removal (F = 0.052, p = 0.82). The effectiveness of the process was influenced the most by the type of biochar and, to a lesser extent, by its dosage. Statistical analysis also showed an interaction between the type of solution and the dosage, the type of solution and the type of biochar, and the dosage and the type of biochar (Table 5). Only for the control sample and hot-water-modified and KOH-modified biochar for both the filtrate and the synthetic solution, the process efficiency was improved as the sorbent dosage increased. Furthermore, there was no statistical difference in the degree of ammonium nitrogen removal for the highest dosages of the mentioned modified biochar variants (according to Tukey's test, they were classified in the same groups).

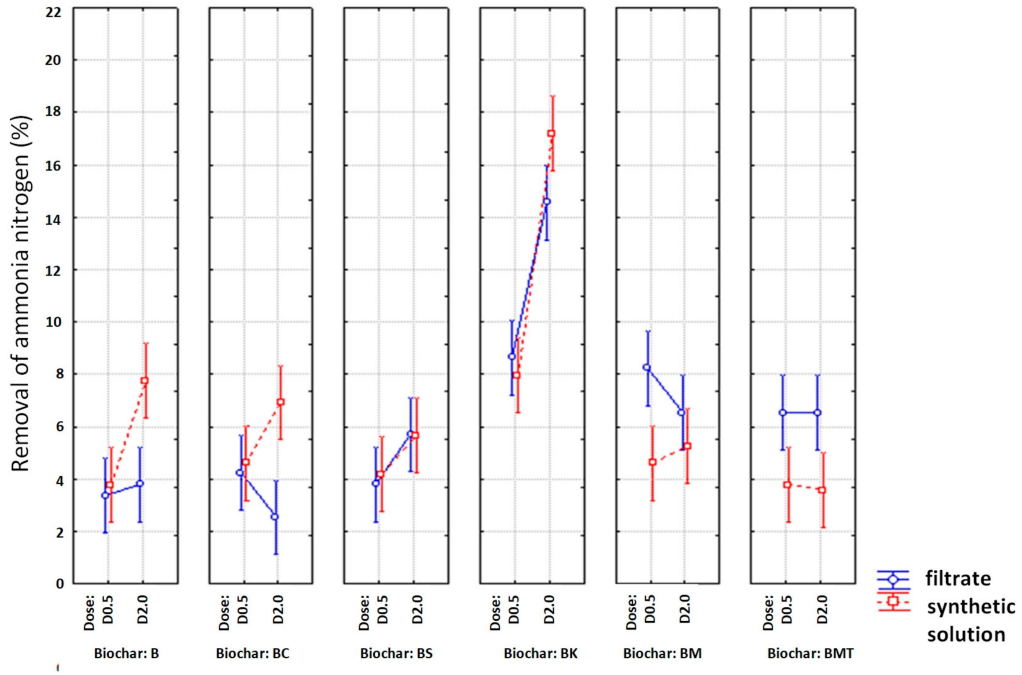


Figure 4. Removal of ammonia nitrogen.

Table 5. Results of factorial ANOVA for removal of ammonia nitrogen.

Factors	F	p
solution	0.052	0.821128
dose	41.060	0.000000
biochar	68.035	0.000000
solution × dose	13.056	0.000722
solution × biochar	10.228	0.000001
dose × biochar	17.783	0.000000
solution × dose × biochar	1.890	0.113642

In turn, for BC, after increasing the dosage from 0.5 to 2.0 g, there was an increase in the efficiency of ammonium nitrogen removal for the model solution, whereas for the filtrate, this trend was reversed. The modification of biochar with magnesium chloride for both dosages in the case of the filtrate allowed an increase in the process efficiency compared to the control sample (unmodified biochar). In turn, for the synthetic solution, a higher degree of ammonium nitrogen removal was observed for the control sample only for a dosage of 0.5 g BM. For both solutions, increasing the amount of BMT in the medium did not increase the degree of ammonium nitrogen removal (averages in the same

groups-according to Tukey's test). However, it should be noted that the efficiency of the process was higher for the filtrate (Figure 4).

Increasing the biochar dosage from 0.5 to 2 g significantly decreased ammonium nitrogen adsorption efficiency. Bai et al. [22] noted a similar phenomenon. According to the mentioned authors, the reduction in adsorption capacity with the increase in biochar dosage may be linked with the fact that many surface areas provided increased adsorption sites for the ammonium ions to adhere to, which leads to an increase in the competition for ammonium. The same trend was observed by Zhang et al. [60] and Zhao et al. [61] with regard to zeolites. The highest adsorption capacity of ammonium nitrogen was recorded for KOH-modified biochar. For this biochar, the adsorption capacity of the filtrate and the model solution for the 0.5 g dosage was 15.31 mg/g and 14.19 mg/g, respectively, while for the 2.0 g dosage, it was 6.40 mg/g and 7.65 mg/g (Table 4). A similar result to the presented ones was obtained by Bai et al. [22] who used fecal biochar produced at 600 °C and then demineralized HCl (2 mol/L) to remove ammonium nitrogen from urine and a synthetic solution. For them, the adsorption capacity was 17.5 mg/g and was obtained at a biochar dosage of 5 g/L.

On the other hand, the ability to remove N-NH_4^+ from the filtrate and the synthetic solution for non-modified biochar was significantly lower at 5.97 mg/g and 6.72 mg/g (for 0.5 g dosage) and 1.68 mg/g and 3.45 mg/g (for 2.0 g dosage), respectively. Nevertheless, it is worth noting that the adsorption performance for the control sample was significantly higher than in other works. For example, Tang et al. [24], for biochar produced at 450 °C when removing N-NH_4^+ from municipal wastewater, recorded an adsorption capacity of 1.2 mg/g.

In turn, modifying biochar with magnesium chloride also allowed for a significant increase in adsorption efficiency compared to the control sample (unmodified biochar). The sorption capacity of N-NH_4^+ for the 0.5 g dosage for the filtrate was 14.56 mg/g, and for the synthetic solution, 8.21 mg/g. For BMT biochar, the adsorption capacity was slightly lower at 11.57 mg/g for the filtrate and 6.72 mg/g for the synthetic solution (for 0.5 g dosage). With the increase in dosage, this capacity was reduced for both the filtrate and the synthetic solution. The effects obtained in the work with regard to modification with magnesium chloride are lower than those reported in the literature. For example, Jiang et al., [23] for six biochar variants made from different substrates and subsequently modified with $MgCl_2$, recorded the highest adsorption capacity of 24.04 mg/g (0.25 g dosage), i.e., for samples with the most significant specific surface area, volume, and pore size and relatively high magnesium content among the tested.

Other biochar modifications made using physical methods had a lesser impact on the adsorption efficiency than the control sample. With BC and BS biochar variants, the adsorption capacity for the 0.5 g dosage ranged from 6.7.2 to 8.21 mg/g and 1.12 to 3.08 mg/g, respectively, for the filtrate and the synthetic solution.

In contrast to ammonium nitrogen, orthophosphate ions have a significant statistical effect on the solution type and the degree of removal (F = 170.6, p = 0.000). However, as the factor analysis of variance showed, the dosage of biochar influenced the effectiveness of ion removal to the greatest extent; the type of biochar did that to a lesser extent. There was also an interaction between the variables defined in the statistical analysis (Table 6). The highest ion removal was recorded for KOH-modified biochar (BK) for the filtrate and the stock solution (Figure 5). The percentage of phosphorus removal was 29.90% and 38.89%, respectively, for the 0.5 g dosage and for the 2 g dosage, 71.87% and 85.58%, respectively. By contrast, the adsorption capacity (Table 4) for BK was 12.02 mg/g and 13.35 mg/g for the filtrate and the synthetic solution, respectively, and was thus significantly higher than for the control sample. In general, with the increase in dosage, improvements in process efficiency were noted. A deviation from the rule was noted only for BMT biochar.

Table 6. Results of factorial ANOVA for removal of phosphorus.

Factors	F	*p*
solution	170.5697	0.000000
dose	602.2890	0.000000
biochar	383.0134	0.000000
solution × dose	22.1578	0.000022
solution × biochar	9.2743	0.000003
dose × biochar	35.1475	0.000000
solution × dose × biochar	6.2098	0.000162

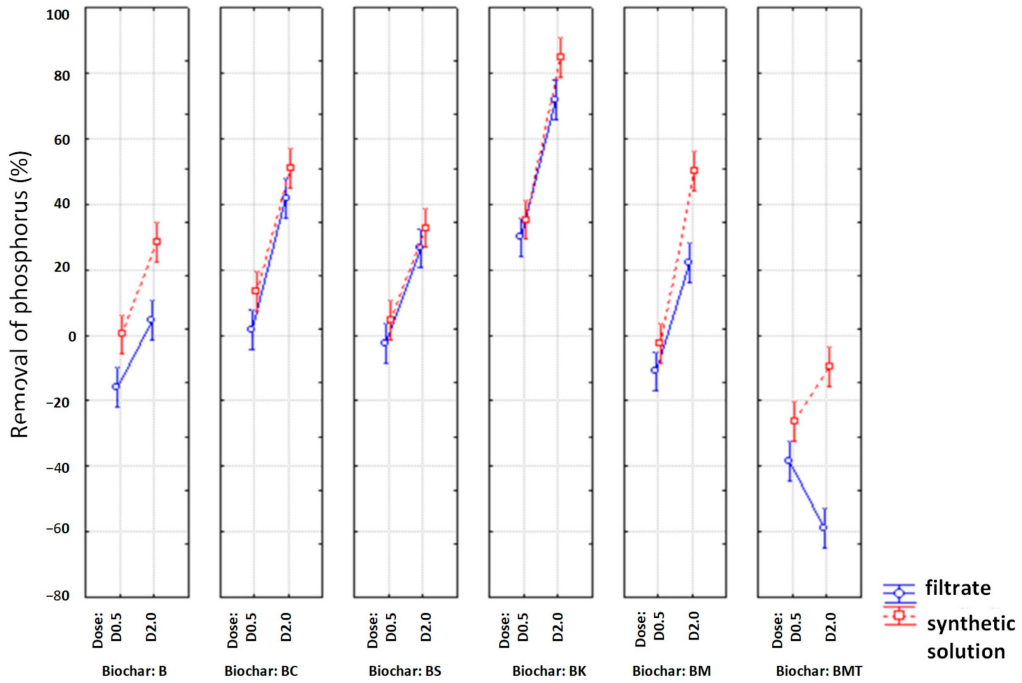


Figure 5. Removal of phosphorus.

As compiled in Table 4, adsorption performance could not be estimated only for some biochar variants. In particular, this trend was evident with regard to the filtrate, which may be directly related to the nature of the matrix and, consequently, to the presence of other ions competing with orthophosphate ions [29]. It is also worth noting that for these biochar variants, leaching of phosphorus compounds has been observed, resulting in an increase in the concentration of phosphorus in real and synthetic solutions. The observed trend was the strongest in $MgCl_2$-modified biochar samples. With these biochar variants, only for the 2.0 dosage, the adsorption capacity has been calculated. For the filtrate, it was 2.22 mg/g and for the synthetic solution, it was 4.74 mg/g. It is surprising as, in most cases, the use of magnesium compounds allows for an increase on the surface of the biochar in the amount of colloidal and nano-sized structures of periclase, which show a strong ability to bind phosphates from aqueous solutions [62]. Numerous studies confirm this. For example, the authors of [23] studied the effect of biochar modification with $MgCl_2$ on phosphorus removal efficiency. The authors noted the highest value of sorption capacity P for a dosage of 0.25 g, which was 31 mg/g. The effectiveness was strongly correlated with the Mg content in biochar, to a lesser degree, with the specific surface area and volume of pores. Also, Xu et al. [63], after using magnesium oxide, noted improvements in the removal of ammonium and orthophosphate ions from solutions. According to [64–66], the calcium, magnesium, and iron content performs a key role in reducing phosphorus levels in the purified medium. This phenomenon occurs because metals can sorb orthophosphate ions via surface deposition.

Comparing the results obtained to literature data is extremely difficult. This is because the properties of biochar and, consequently, the effectiveness of the removal of selected impurities are influenced by many factors. The most important are the type of biomass, the source of its origin, the conditions of pyrolysis, the method of modification of the biochar, its quantity, the time of contact, and the concentration of ions in the solution (Table 7). The significantly higher adsorption efficiency for the synthetic solution is not surprising and is caused by the lack of other ions in the solution that could compete for active sites with ammonium nitrogen or orthophosphate ions. The observation is confirmed by, among others, Kizito et al. [67] or studies by Liu et al. [68], which showed that the negative effect on adsorption of ammonium nitrogen ions is present in the solution of Al^{3+}, Zn^{2+}, HCO^{3-}, $PO_4{}^{3-}$ ions. Adsorption of orthophosphate ions, on the other hand, may be adversely affected by the presence of chlorine ions [69] or other ions competing with them for active sites in biochar [70]. Precipitation of ions present in the solution may also occur, reducing biochar's porosity. However, it should be emphasized that the adsorption efficiency is not always higher in synthetic solutions. For example, Sarhot et al. [71] reported better results for dairy slurry, which is associated with a positive effect of organic matter on the sorption process.

Table 7. The effect of biochar removal of ammonia nitrogen and phosphorus from aqueous solutions.

Type of Feedstock	Pyrolysis Temperature °C	Treatment (Modification) Method	Biochar Dose g	Initial Concentration mg/L	Adsorption Capacity mg/g	Reference
		$NH_4{}^+$				
Pine sawdust	300	pristine	3	100	5.38	[62]
Wheat straw	550	pristine	3	100	2.08	
Wood waste	600	MgO	2	8203	47.5	
Sugarcane harvest residue	550	MgO	1.25	200	22	
Oak sawdust	300	-	0.1	25.7	3.12	[72]
		$LaCl_3$			4.13	
Mixed hardwood	300	-	2	980	2.8	[71]
		-	2	713 (dairy manure)	5.3	
Corn cob	400	-	-	100	1.09	[73]
Corn cob	600	-	-	100	0.69	
		$PO_4{}^{2-}$				
Wood waste	600	MgO	2	318.5	116.40 ($PO_4{}^2$)	[62]
Bamboo	600	Mg-Al layered double hydroxide	2	50	13.11 ($PO_4{}^{2-}$)	
Sugar beet tailings	600	$MgCl_2$ solution immersed	2	1600	135.00 ($PO_4{}^{2-}$)	
Sesame straw	600	$ZnCl_2$	0.1	20 (P)	9.39	[74]
		MgO	0.1		8.42	
Thalia dealbata	500	CO_2 at 500 °C	0.2	30	2.9	[75]
	500	CO_2 at 600 °C	0.2		38.12	
Sugar beet tailings	600	$MgCl_2$	0.1	20	66.7	[76]
Pine wood	600	$MgCl_2$	0.1	20	0.5	
Mixed hardwood	300	-	2	24	0.48	[72]
	300	-	2	24 (dairy manure)	0.24	
Cotton stalks	350	immobilization of ferric oxides on the biochar granule	2	20	0.963	[77]
		$FeCl_3$, then granulation	2		0.399	
		chemical precipitation of ferric oxide on biochar	2		0.319	

The pH of the solution has a significant impact on the effectiveness of the removal of impurities, as it affects the ion exchange in the solution and its ionic form. In the case of

ammonium nitrogen, a too high pH (>8), as shown by the Kizito et al. [67] studies, may result in a decrease in adsorption (the effect of an increase in the free ammonia content in the solution that is not adsorbed on the surface of the sorbent). The phenomenon can also be observed at a too-low pH (<4), and then there is competition at active sites between hydrogen ions and ammonium nitrogen ions [47]. In the case of phosphates, on the other hand, the pH of the solution determines the distribution of phosphate forms. In a strongly alkaline environment, PO_4^{3-} dominates, which is very poorly adsorbed on the surface of the sorbent. Aside from that, there is competition with OH^- ions. According to [78], the most preferred form of phosphorus adsorption in orthophosphates is H_2PO_4 (dominating at a pH of approximately 4). The charge of biochar is also not insignificant. Positive promotes adsorption of anions due to electrostatic interactions between sorbent and ions. For the reasons described in the paragraph, taking into consideration the pH of the solutions after the addition of biochar to them, it was decided to adjust their pH to 4.0 (Figure 6). As expected, the pH was most affected by the type of solution and, to a lesser extent, the dosage and type of biochar. It should be noted that interaction has been observed for all variables (Table 8).

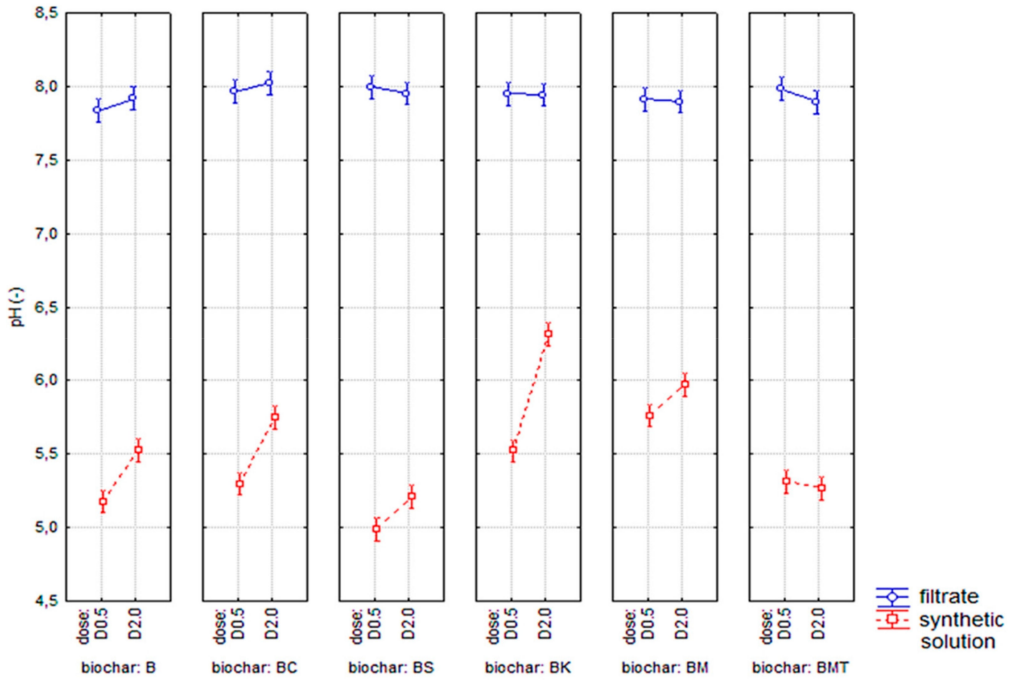


Figure 6. pH before correction pH.

Table 8. Results of factorial ANOVA for pH before correction pH.

Factors	F	*p*
solution	24355.3	0
dose	109.9	0
biochar	71.4	0
solution × dose	113.7	0
solution × biochar	78.7	0
dose × biochar	17.5	0
solution × dose × biochar	11.1	0

After the adsorption process, there was an increase in the pH of the solutions compared to the samples before the pH correction. This trend was more pronounced in the synthetic solution (Figure 7). The statistical analysis showed that, in the case of the filtrate, the pH was the most affected by the dosage of biochar and, to a lesser extent, by its type. On the other hand, the reverse trend has been observed for the model solution (Table 9).

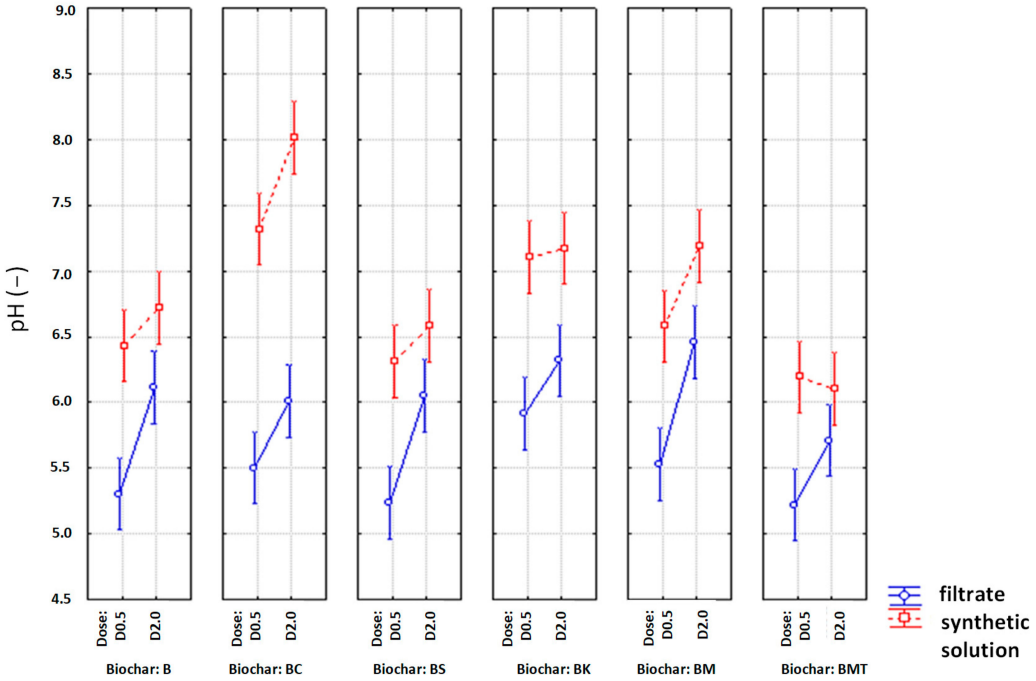


Figure 7. pH after the batch test.

Table 9. Results of factorial ANOVA for pH.

	Filtrate				Synthetic Solution			
	pH before		pH after		pH before		pH after	
Factors	**F**	***p***	**F**	***p***	**F**	***p***	**F**	***p***
type of biochar	13	0.000004	3.17	0.024491	82.1	0.000000	379.0	0.000000
Dose biochar	0	0.781917	36.68	0.000003	124.4	0.000000	182.2	0.000000
type of biochar × Dose biochar	7	0.000400	0.67	0.652760	15.1	0.000001	29.2	0.000000

4. Conclusions

The production efficiency of biochar variants was closely linked to the temperature at which they were produced.

(1) The increase in temperature caused a decrease in the yield of biochar. There was a 21% reduction in the parameter when comparing the extreme tested in research temperatures from 62.41% to 49.33% for temperatures of 400 and 700 °C, respectively. A similar trend was observed for carbon (36% reduction, from 42.4% to 27.0%), hydrogen (66% reduction, from 3.22% to 1.4%), and nitrogen content and H/C (64% reduction, from 0.73% to 0.26%) in biochar.

(2) An increase in the pyrolysis temperature of the digestate resulted in an increase in the biochar pH, ash content and BET surface area. The parameters mentioned above increased, respectively, from 7.13 to 11, 48.13 to 71.43 and from 11.09 to 45.53 m^2/g.

(3) The pyrolysis temperature influenced the change in the type and quantity of surface functional groups. A decreasing number of acidic functional groups and increasing aromaticity of biochar were observed.

The experiments conducted proved that the pyrolysis of digestate can produce biochar which can be used to pre-treat filtrate from dewatering of digestate. However, obtaining an effective sorbent requires its modification. In our research, the best results were obtained for biochar modified with potassium hydroxide. For this trial, 15%/17% (filtrate/synthetic model solution) and 72%/86% nitrogen and phosphorus removal, respectively, were achieved.

The obtained results show that, despite the increasing number of publications on the use of biochar as a sorbent, there are still gaps that need to be filled, particularly in modifying the biochar produced for its practical application. The study results presented in this article indicate the high potential of post-treatment biochar as a tool for producing biochar dedicated for use in wastewater treatment plants. In wastewater treatment plants, it appears that biochar, aimed at producing/forming the right functional groups, can contribute to reducing the load of phosphorus and nitrogen returned to the wastewater treatment plant with the filtrate from under the presses, thereby complying with increasingly restrictive wastewater treatment legislation. However, this does not change the fact that further research is needed into the possibility of using biochar with adsorbed ions as slow-release fertilizers in agriculture or horticulture, especially with regard to phosphorus. Using sludge-based sorbents and the nutrients retained on them as soil improvers may be an interesting solution to "close the nutrient cycle". This can contribute to the growth of cultured biomass [1]. Moreover, as research by El Sharkawi et al. [79] shows, such slow-release fertilizers used on sandy soils are more effective than mineral fertilizers. They reduce nitrogen losses while increasing the efficiency of their use in plant growth. It is equally important to increase carbon storage in the soil. It is also worth determining how biochar modification may affect the anaerobic digestion process, its efficiency, stability and whether the produced biochar can be used for biogas upgrading.

Author Contributions: Conceptualization, K.W. and A.G.; methodology, K.W. and A.G.; software, K.W. and A.G.; validation, K.W. and A.G.; formal analysis, K.W. and A.G.; investigation, K.W. and A.G.; resources, K.W. and A.G.; data curation, K.W. and A.G.; writing—original draft preparation, K.W. and A.G; writing—review and editing, K.W. and A.G.; visualization, K.W. and A.G.; supervision, K.W. and A.G.; project administration, K.W. and A.G.; funding acquisition, K.W. and A.G. All authors have read and agreed to the published version of the manuscript.

Funding: The scientific research was funded by the statute subvention of Czestochowa University of Technology (Faculty of Infrastructure and Environment)–BS/PB-400-301/24.

Data Availability Statement: Data are contained within the article.

Acknowledgments: The authors gratefully acknowledge technical support from Lucyna Gądek.

Conflicts of Interest: The authors declare no conflict of interest.

References

1. Barber, S.T.; Yin, J.; Draper, K.; Trabold, T.A. Closing Nutrient Cycles with Biochar—From Filtration to Fertilizer. *J. Clean. Prod.* **2018**, *197*, 1597–1606. [CrossRef]
2. Jin, J.; Wang, M.; Cao, Y.; Wu, S.; Liang, P.; Li, Y.; Zhang, J.; Zhang, J.; Wong, M.H.; Shan, S.; et al. Cumulative Effects of Bamboo Sawdust Addition on Pyrolysis of Sewage Sludge: Biochar Properties and Environmental Risk from Metals. *Bioresour. Technol.* **2017**, *228*, 218–226. [CrossRef] [PubMed]
3. Agyarko-Mintah, E.; Cowie, A.; Singh, B.P.; Joseph, S.; Van Zwieten, L.; Cowie, A.; Harden, S.; Smillie, R. Biochar Increases Nitrogen Retention and Lowers Greenhouse Gas Emissions When Added to Composting Poultry Litter. *Waste Manag.* **2017**, *61*, 138–149. [CrossRef] [PubMed]
4. Liu, H.; Dong, Y.; Wang, H.; Liu, Y. Ammonium Adsorption from Aqueous Solutions by Strawberry Leaf Powder: Equilibrium, Kinetics and Effects of Coexisting Ions. *Desalination* **2010**, *263*, 70–75. [CrossRef]
5. Mia, S.; Uddin, M.E.; Kader, M.A.; Ahsan, A.; Mannan, M.A.; Hossain, M.M.; Solaiman, Z.M. Pyrolysis and Co-Composting of Municipal Organic Waste in Bangladesh: A Quantitative Estimate of Recyclable Nutrients, Greenhouse Gas Emissions, and Economic Benefits. *Waste Manag.* **2018**, *75*, 503–513. [CrossRef]
6. Sanchez-Monedero, M.A.; Cayuela, M.L.; Roig, A.; Jindo, K.; Mondini, C.; Bolan, N. Role of Biochar as an Additive in Organic Waste Composting. *Bioresour. Technol.* **2018**, *247*, 1155–1164. [CrossRef] [PubMed]
7. Mohan, D.; Rajput, S.; Singh, V.K.; Steele, P.H.; Pittman, C.U. Modeling and Evaluation of Chromium Remediation from Water Using Low Cost Bio-Char, a Green Adsorbent. *J. Hazard. Mater.* **2011**, *188*, 319–333. [CrossRef] [PubMed]
8. Agegnehu, G.; Srivastava, A.K.; Bird, M.I. The Role of Biochar and Biochar-Compost in Improving Soil Quality and Crop Performance: A Review. *Appl. Soil Ecol.* **2017**, *119*, 156–170. [CrossRef]
9. Zama, E.F.; Zhu, Y.G.; Reid, B.J.; Sun, G.X. The Role of Biochar Properties in Influencing the Sorption and Desorption of Pb(II), Cd(II) and As(III) in Aqueous Solution. *J. Clean. Prod.* **2017**, *148*, 127–136. [CrossRef]

10. Ferreira, S.D.; Manera, C.; Silvestre, W.P.; Pauletti, G.F.; Altafini, C.R.; Godinho, M. Use of Biochar Produced from Elephant Grass by Pyrolysis in a Screw Reactor as a Soil Amendment. *Waste Biomass Valorization* **2019**, *10*, 3089–3100. [CrossRef]
11. Franciski, M.A.; Peres, E.C.; Godinho, M.; Perondi, D.; Foletto, E.L.; Collazzo, G.C.; Dotto, G.L. Development of CO_2 Activated Biochar from Solid Wastes of a Beer Industry and Its Application for Methylene Blue Adsorption. *Waste Manag.* **2018**, *78*, 630–638. [CrossRef]
12. Godlewska, P.; Schmidt, H.P.; Ok, Y.S.; Oleszczuk, P. Biochar for Composting Improvement and Contaminants Reduction. A Review. *Bioresour. Technol.* **2017**, *246*, 193–202. [CrossRef]
13. Ahmad, M.; Lee, S.S.; Dou, X.; Mohan, D.; Sung, J.K.; Yang, J.E.; Ok, Y.S. Effects of Pyrolysis Temperature on Soybean Stover- and Peanut Shell-Derived Biochar Properties and TCE Adsorption in Water. *Bioresour. Technol.* **2012**, *118*, 536–544. [CrossRef]
14. Liu, W.; Huo, R.; Xu, J.; Liang, S.; Li, J.; Zhao, T.; Wang, S. Effects of Biochar on Nitrogen Transformation and Heavy Metals in Sludge Composting. *Bioresour. Technol.* **2017**, *235*, 43–49. [CrossRef] [PubMed]
15. Li, S.; Chen, G. Thermogravimetric, Thermochemical, and Infrared Spectral Characterization of Feedstocks and Biochar Derived at Different Pyrolysis Temperatures. *Waste Manag.* **2018**, *78*, 198–207. [CrossRef] [PubMed]
16. Song, W.; Guo, M. Quality Variations of Poultry Litter Biochar Generated at Different Pyrolysis Temperatures. *J. Anal. Appl. Pyrolysis* **2012**, *94*, 138–145. [CrossRef]
17. Wystalska, K.; Malińska, K.; Włodarczyk, R.; Chajczyk, O. Effects of Pyrolysis Parameters on the Yield and Properties of Biochar from Pelletized Sunflower Husk. *E3S Web Conf.* **2018**, *44*, 00197. [CrossRef]
18. Vaughn, S.F.; Dinelli, F.D.; Kenar, J.A.; Jackson, M.A.; Thomas, A.J.; Peterson, S.C. Physical and Chemical Properties of Pyrolyzed Biosolids for Utilization in Sand-Based Turfgrass Rootzones. *Waste Manag.* **2018**, *76*, 98–105. [CrossRef] [PubMed]
19. Wystalska, K.; Malińska, K.; Barczak, M. Poultry Manure Derived Biochars—The Impact of Pyrolysis Temperature on Selected Properties and Potentials for Further Modifications. *J. Sustain. Dev. Energy Water Environ. Syst.* **2021**, *9*, 1080337. [CrossRef]
20. Zhao, B.; O'Connor, D.; Zhang, J.; Peng, T.; Shen, Z.; Tsang, D.C.W.; Hou, D. Effect of Pyrolysis Temperature, Heating Rate, and Residence Time on Rapeseed Stem Derived Biochar. *J. Clean. Prod.* **2018**, *174*, 977–987. [CrossRef]
21. Zhang, H.; Chen, C.; Gray, E.M.; Boyd, S.E. Effect of Feedstock and Pyrolysis Temperature on Properties of Biochar Governing End Use Efficacy. *Biomass Bioenergy* **2017**, *105*, 136–146. [CrossRef]
22. Bai, X.; Li, Z.; Zhang, Y.; Ni, J.; Wang, X.; Zhou, X. Recovery of Ammonium in Urine by Biochar Derived from Faecal Sludge and Its Application as Soil Conditioner. *Waste Biomass Valorization* **2018**, *9*, 1619–1628. [CrossRef]
23. Jiang, Y.H.; Li, A.Y.; Deng, H.; Ye, C.H.; Wu, Y.Q.; Linmu, Y.D.; Hang, H.L. Characteristics of Nitrogen and Phosphorus Adsorption by Mg-Loaded Biochar from Different Feedstocks. *Bioresour. Technol.* **2019**, *276*, 183–189. [CrossRef]
24. Tang, Y.; Alam, M.S.; Konhauser, K.O.; Alessi, D.S.; Xu, S.; Tian, W.J.; Liu, Y. Influence of Pyrolysis Temperature on Production of Digested Sludge Biochar and Its Application for Ammonium Removal from Municipal Wastewater. *J. Clean. Prod.* **2019**, *209*, 927–936. [CrossRef]
25. Mu'azu, N.D.; Jarrah, N.; Zubair, M.; Alagha, O. Removal of Phenolic Compounds from Water Using Sewage Sludge-Based Activated Carbon Adsorption: A Review. *Int. J. Environ. Res. Public Health* **2017**, *14*, 1094. [CrossRef]
26. Xu, G.; Yang, X.; Spinosa, L. Development of Sludge-Based Adsorbents: Preparation, Characterization, Utilization and Its Feasibility Assessment. *J. Environ. Manag.* **2015**, *151*, 221–232. [CrossRef] [PubMed]
27. Devi, P.; Saroha, A.K. Utilization of Sludge Based Adsorbents for the Removal of Various Pollutants: A Review. *Sci. Total Environ.* **2017**, *578*, 16–33. [CrossRef] [PubMed]
28. Xu, D.; Cao, J.; Li, Y.; Howard, A.; Yu, K. Effect of Pyrolysis Temperature on Characteristics of Biochars Derived from Different Feedstocks: A Case Study on Ammonium Adsorption Capacity. *Waste Manag.* **2019**, *87*, 652–660. [CrossRef]
29. Dai, Y.; Wang, W.; Lu, L.; Yan, L.; Yu, D. Utilization of Biochar for the Removal of Nitrogen and Phosphorus. *J. Clean. Prod.* **2020**, *257*, 120573. [CrossRef]
30. Gajewska, M.; Obarska-Pempkowiak, H. Effect of Recycling of Reject Waters from Dewatering the Sludges on the Operation Efficiency of a Wastewater Treatment Plant. *Przem. Chem.* **2008**, *87*, 448–451.
31. Tayibi, S.; Monlau, F.; Bargaz, A.; Jimenez, R.; Barakat, A. Synergy of Anaerobic Digestion and Pyrolysis Processes for Sustainable Waste Management: A Critical Review and Future Perspectives. Renew. *Sustain. Energy Rev.* **2021**, *152*, 111603. [CrossRef]
32. Sobik-Szołtysek, J.; Bień, J.; Grosser, A. Assessment of the Sorption Properties of Materials Proposed for the Construction of Insulation Barriers. *Environ. Prot. Eng.* **2016**, *42*, 169–189. [CrossRef]
33. *PN-EN ISO 18122:2016-01*; Solid Biofuels—Determination of Ash Content. Polish Committee for Standardization: Warsaw, Poland, 2016.
34. *PN-EN 16169:2012*; Sewage Sludge. Treated Bio-Waste and Soil. Determination of Nitrogen by the Kjeldahl Method. Polish Committee for Standardization: Warsaw, Poland, 2012.
35. APHA. *Standard Methods for the Examination of Water and Wastewater*; American Public Health Association: Washington, DC, USA, 1999.
36. Llorach-Massana, P.; Lopez-Capel, E.; Peña, J.; Rieradevall, J.; Montero, J.I.; Puy, N. Technical Feasibility and Carbon Footprint of Biochar Co-Production with Tomato Plant Residue. *Waste Manag.* **2017**, *67*, 121–130. [CrossRef] [PubMed]
37. Dunnigan, L.; Morton, B.J.; Ashman, P.J.; Zhang, X.; Kwong, C.W. Emission Characteristics of a Pyrolysis-Combustion System for the Co-Production of Biochar and Bioenergy from Agricultural Wastes. *Waste Manag.* **2018**, *77*, 59–66. [CrossRef] [PubMed]

38. Tomczyk, A.; Sokołowska, Z.; Boguta, P. Biochar Physicochemical Properties: Pyrolysis Temperature and Feedstock Kind Effects. *Rev. Environ. Sci. Biotechnol.* **2020**, *19*, 191–215. [CrossRef]
39. Ruiz-Gómez, N.; Quispe, V.; Ábrego, J.; Atienza-Martínez, M.; Murillo, M.B.; Gea, G. Co-Pyrolysis of Sewage Sludge and Manure. *Waste Manag.* **2017**, *59*, 211–221. [CrossRef] [PubMed]
40. Mohan, D.; Pittman, C.U.; Steele, P.H. Pyrolysis of Wood/Biomass for Bio-Oil: A Critical Review. *Energy Fuels* **2006**, *20*, 848–889. [CrossRef]
41. Version, D.; Wildt, D. *Biomass Pyrolysis for Chemicals de Wildt, Paulus*; University of Groningen: Groningen, The Netherlands, 2011; ISBN 9789036749947.
42. Brown, R.; Lehmann, J.; Joseph, S. *Biochar for Environmental Management: Science and Technology*; Earthscan: London, UK, 2009; Volume 8, pp. 127–146.
43. Ahmad, M.; Lee, S.S.; Lim, J.E.; Lee, S.E.; Cho, J.S.; Moon, D.H.; Hashimoto, Y.; Ok, Y.S. Speciation and Phytoavailability of Lead and Antimony in a Small Arms Range Soil Amended with Mussel Shell, Cow Bone and Biochar: EXAFS Spectroscopy and Chemical Extractions. *Chemosphere* **2014**, *95*, 433–441. [CrossRef]
44. Ding, W.; Dong, X.; Ime, I.M.; Gao, B.; Ma, L.Q. Pyrolytic Temperatures Impact Lead Sorption Mechanisms by Bagasse Biochars. *Chemosphere* **2014**, *105*, 68–74. [CrossRef]
45. Chen, T.; Zhang, Y.; Wang, H.; Lu, W.; Zhou, Z.; Zhang, Y.; Ren, L. Influence of Pyrolysis Temperature on Characteristics and Heavy Metal Adsorptive Performance of Biochar Derived from Municipal Sewage Sludge. *Bioresour. Technol.* **2014**, *164*, 47–54. [CrossRef]
46. Zhao, S.X.; Ta, N.; Wang, X.D. Effect of Temperature on the Structural and Physicochemical Properties of Biochar with Apple Tree Branches as Feedstock Material. *Energies* **2017**, *10*, 1293. [CrossRef]
47. Novak, J.M.; Lima, I.; Xing, B.; Gaskin, J.W.; Steiner, C.; Das, K.C.; Ahmedna, M.; Rehrah, D.; Watts, D.W.; Busscher, W.J. Characterization of Designer Biochar Produced at Different Temperatures and Their Effects on a Loamy Sand. *Ann. Environ. Sci.* **2009**, *3*, 195–206.
48. Schmidt, H.P.; Bucheli, T.; Kammann, C.; Glaser, B.; Abiven, S.; Leifeld, J. *European Biochar Certificate—Guidelines for a Sustainable Production of Biochar*; European Biochar Foundation (EBC): Arbaz, Switzerland, 2012.
49. De Bhowmick, G.; Sarmah, A.K.; Sen, R. Production and Characterization of a Value Added Biochar Mix Using Seaweed, Rice Husk and Pine Sawdust: A Parametric Study. *J. Clean. Prod.* **2018**, *200*, 641–656. [CrossRef]
50. Zolfi Bavariani, M.; Ronaghi, A.; Ghasemi, R. Influence of Pyrolysis Temperatures on FTIR Analysis, Nutrient Bioavailability, and Agricultural Use of Poultry Manure Biochars. *Commun. Soil Sci. Plant Anal.* **2019**, *50*, 402–411. [CrossRef]
51. Qi, F.; Yan, Y.; Lamb, D.; Naidu, R.; Bolan, N.S.; Liu, Y.; Ok, Y.S.; Donne, S.W.; Semple, K.T. Thermal Stability of Biochar and Its Effects on Cadmium Sorption Capacity. *Bioresour. Technol.* **2017**, *246*, 48–56. [CrossRef]
52. Srinivasan, P.; Sarmah, A.K.; Smernik, R.; Das, O.; Farid, M.; Gao, W. A Feasibility Study of Agricultural and Sewage Biomass as Biochar, Bioenergy and Biocomposite Feedstock: Production, Characterization and Potential Applications. *Sci. Total Environ.* **2015**, *512–513*, 495–505. [CrossRef]
53. Zhang, J.; Lü, F.; Zhang, H.; Shao, L.; Chen, D.; He, P. Multiscale Visualization of the Structural and Characteristic Changes of Sewage Sludge Biochar Oriented towards Potential Agronomic and Environmental Implication. *Sci. Rep.* **2015**, *5*, 9406. [CrossRef]
54. Sharma, R.K.; Wooten, J.B.; Baliga, V.L.; Martoglio-Smith, P.A.; Hajaligol, M.R. Characterization of Char from the Pyrolysis of Tobacco. *J. Agric. Food Chem.* **2002**, *50*, 771–783. [CrossRef]
55. Hung, C.Y.; Tsai, W.T.; Chen, J.W.; Lin, Y.Q.; Chang, Y.M. Characterization of Biochar Prepared from Biogas Digestate. *Waste Manag.* **2017**, *66*, 53–60. [CrossRef] [PubMed]
56. Li, H.; Dong, X.; da Silva, E.B.; de Oliveira, L.M.; Chen, Y.; Ma, L.Q. Mechanisms of Metal Sorption by Biochars: Biochar Characteristics and Modifications. *Chemosphere* **2017**, *178*, 466–478. [CrossRef] [PubMed]
57. Hasnan, F.I.; Iamail, K.N.; Musa, M.; Jaapar, J.; Alwi, H.; Hamid, K.K.K. Characterization of Bio Char Derived from Tapioca Skin. *IOP Conf. Ser. Mater. Sci. Eng.* **2018**, *334*, 12016. [CrossRef]
58. Lee, J.Y.; Lee, K.K. A Short Note on Investigation and Remediation of Contaminated Groundwater and Soil in Korea. *J. Eng. Geol.* **2004**, *14*, 123–130.
59. Li, J.; Cao, L.; Yuan, Y.; Wang, R.; Wen, Y.; Man, J. Comparative Study for Microcystin-LR Sorption onto Biochars Produced from Various Plant- and Animal-Wastes at Different Pyrolysis Temperatures: Influencing Mechanisms of Biochar Properties. *Bioresour. Technol.* **2018**, *247*, 794–803. [CrossRef] [PubMed]
60. Zhang, M.; Zhang, H.; Xu, D.; Han, L.; Niu, D.; Tian, B.; Zhang, J.; Zhang, L.; Wu, W. Removal of Ammonium from Aqueous Solutions Using Zeolite Synthesized from Fly Ash by a Fusion Method. *Desalination* **2011**, *271*, 111–121. [CrossRef]
61. Zhao, Y.; Zhang, B.; Zhang, X.; Wang, J.; Liu, J.; Chen, R. Preparation of Highly Ordered Cubic NaA Zeolite from Halloysite mineral for Adsorption of Ammonium Ions. *J. Hazard. Mater.* **2010**, *178*, 658–664. [CrossRef] [PubMed]
62. Xiang, W.; Zhang, X.; Chen, J.; Zou, W.; He, F.; Hu, X.; Tsang, D.C.W.; Ok, Y.S.; Gao, B. Biochar Technology in Wastewater Treatment: A Critical Review. *Chemosphere* **2020**, *252*, 126539. [CrossRef] [PubMed]
63. Xu, K.; Lin, F.; Dou, X.; Zheng, M.; Tan, W.; Wang, C. Recovery of Ammonium and Phosphate from Urine as Value-Added Fertilizer Using Wood Waste Biochar Loaded with Magnesium Oxides. *J. Clean. Prod.* **2018**, *187*, 205–214. [CrossRef]
64. Yin, Q.; Zhang, B.; Wang, R.; Zhao, Z. Biochar as an Adsorbent for Inorganic Nitrogen and Phosphorus Removal from Water: A Review. *Environ. Sci. Pollut. Res.* **2017**, *24*, 26297–26309. [CrossRef]

65. Melia, P.M.; Busquets, R.; Hooda, P.S.; Cundy, A.B.; Sohi, S.P. Driving Forces and Barriers in the Removal of Phosphorus from Water Using Crop Residue, Wood and Sewage Sludge Derived Biochars. *Sci. Total Environ.* **2019**, *675*, 623–631. [CrossRef]
66. Zhang, L.; Deng, F.; Liu, Z.; Ai, L. Removal of Ammonia Nitrogen and Phosphorus by Biochar Prepared from Sludge Residue after Rusty Scrap Iron and Reduced Iron Powder Enhanced Fermentation. *J. Environ. Manag.* **2021**, *282*, 111970. [CrossRef]
67. Kizito, S.; Wu, S.; Kipkemoi Kirui, W.; Lei, M.; Lu, Q.; Bah, H.; Dong, R. Evaluation of Slow Pyrolyzed Wood and Rice Husks Biochar for Adsorption of Ammonium Nitrogen from Piggery Manure Anaerobic Digestate Slurry. *Sci. Total Environ.* **2015**, *505*, 102–112. [CrossRef]
68. Liu, Z.; Zhang, F.S.; Wu, J. Characterization and Application of Chars Produced from Pinewood Pyrolysis and Hydrothermal Treatment. *Fuel* **2010**, *89*, 510–514. [CrossRef]
69. Yao, Y.; Gao, B.; Chen, J.; Yang, L. Engineered Biochar Reclaiming Phosphate from Aqueous Solutions: Mechanisms and Potential Application as a Slow-Release Fertilizer. *Environ. Sci. Technol.* **2013**, *47*, 8700–8708. [CrossRef]
70. Fang, C.; Zhang, T.; Li, P.; Jiang, R.F.; Wang, Y.C. Application of Magnesium Modified Corn Biochar for Phosphorus Removal and Recovery from Swine Wastewater. *Int. J. Environ. Res. Public Health* **2014**, *11*, 9217–9237. [CrossRef]
71. Sarkhot, D.V.; Ghezzehei, T.A.; Berhe, A.A. Effectiveness of Biochar for Sorption of Ammonium and Phosphate from Dairy Effluent. *J. Environ. Qual.* **2013**, *42*, 1545–1554. [CrossRef]
72. Wang, Z.; Guo, H.; Shen, F.; Yang, G.; Zhang, Y.; Zeng, Y.; Wang, L.; Xiao, H.; Deng, S. Biochar Produced from Oak Sawdust by Lanthanum (La)-Involved Pyrolysis for Adsorption of Ammonium (NH_4^+), Nitrate (NO_3^-), and Phosphate (PO_4^{3-}). *Chemosphere* **2015**, *119*, 646–653. [CrossRef]
73. Zhang, Y.; Li, Z.; Mahmood, I.B. Recovery of NH_4^+ by Corn Cob Produced Biochars and Its Potential Application as Soil Conditioner. *Front. Environ. Sci. Eng.* **2014**, *8*, 825–834. [CrossRef]
74. Park, J.H.; Ok, Y.S.; Kim, S.H.; Cho, J.S.; Heo, J.S.; Delaune, R.D.; Seo, D.C. Evaluation of Phosphorus Adsorption Capacity of Sesame Straw Biochar on Aqueous Solution: Influence of Activation Methods and Pyrolysis Temperatures. *Environ. Geochem. Health* **2015**, *37*, 969–983. [CrossRef] [PubMed]
75. Zeng, Z.; Da Zhang, S.; Li, T.Q.; Zhao, F.L.; He, Z.L.; Zhao, H.P.; Yang, X.E.; Wang, H.L.; Zhao, J.; Rafiq, M.T. Sorption of Ammonium and Phosphate from Aqueous Solution by Biochar Derived from Phytoremediation Plants. *J. Zhejiang Univ. Sci. B* **2013**, *14*, 1152–1161. [CrossRef] [PubMed]
76. Yao, Y.; Gao, B.; Inyang, M.; Zimmerman, A.R.; Cao, X.; Pullammanappallil, P.; Yang, L. Biochar Derived from Anaerobically Digested Sugar Beet Tailings: Characterization and Phosphate Removal Potential. *Bioresour. Technol.* **2011**, *102*, 6273–6278. [CrossRef] [PubMed]
77. Ren, J.; Li, N.; Li, L.; An, J.-K.; Zhao, L.; Ren, N.-Q. Granulation and Ferric Oxides Loading Enable Biochar Derived from Cotton Stalk to Remove Phosphate from Water. *Bioresour. Technol.* **2015**, *178*, 119–125. [CrossRef] [PubMed]
78. Loganathan, P.; Vigneswaran, S.; Kandasamy, J.; Bolan, N.S. Removal and Recovery of Phosphate from Water Using Sorption. *Crit. Rev. Environ. Sci. Technol.* **2014**, *44*, 847–907. [CrossRef]
79. El Sharkawi, H.M.; Tojo, S.; Chosa, T.; Malhat, F.M.; Youssef, A.M. Biochar-Ammonium Phosphate as an Uncoated-Slow Release Fertilizer in Sandy Soil. *Biomass Bioenergy* **2018**, *117*, 154–160. [CrossRef]

Disclaimer/Publisher's Note: The statements, opinions and data contained in all publications are solely those of the individual author(s) and contributor(s) and not of MDPI and/or the editor(s). MDPI and/or the editor(s) disclaim responsibility for any injury to people or property resulting from any ideas, methods, instructions or products referred to in the content.